

# TRANSPARENT TESTA GLABRA1 and GLABRA1 Compete for Binding to GLABRA3 in Arabidopsis

Martina Pesch, Ilka Schultheiß, Karsten Klopffleisch, Joachim F. Uhrig, Manfred Koegl, Christoph S. Clemen, Rüdiger Simon, Stefanie Weidtkamp-Peters, and Martin Hülskamp\*

Biocenter, Cologne University, Botanical Institute, 50674 Cologne, Germany (M.P., I.S., K.K., J.F.U., M.H.); Preclinical Target Development and Genomics and Proteomics Core Facilities, German Cancer Research Center, 69120 Heidelberg, Germany (M.K.); Center for Biochemistry, Institute of Biochemistry I, Medical Faculty, Cologne University, 50931 Cologne, Germany (C.S.C.); and Heinrich-Heine Universität Düsseldorf, 40225 Dusseldorf, Germany (R.S., S.W.-P.)

ORCID IDs: 0000-0002-6592-4445 (J.F.H.); 0000-0001-6633-9769 (M.K.); 0000-0002-1317-7716 (R.S.); 0000-0001-7734-3771 (S.W.-P.).

The MBW (for R2R3MYB, basic helix-loop-helix [bHLH], and WD40) genes comprise an evolutionarily conserved gene cassette that regulates several traits such as (pro)anthocyanin and anthocyanin biosynthesis and epidermal cell differentiation in plants. Trichome differentiation in Arabidopsis (*Arabidopsis thaliana*) is governed by GLABRA1 (GL1; R2R3MYB), GL3 (bHLH), and TRANSPARENT TESTA GLABRA1 (TTG1; WD40). They are thought to form a trimeric complex that acts as a transcriptional activation complex. We provide evidence that these three MBW proteins form either GL1 GL3 or GL3 TTG1 dimers. The formation of each dimer is counteracted by the respective third protein in yeast three-hybrid assays, pulldown experiments (luminescence-based mammalian interactome), and fluorescence lifetime imaging microscopy-fluorescence resonance energy transfer studies. We further show that two target promoters, TRIPTYCHON (TRY) and CAPRICE (CPC), are differentially regulated: GL1 represses the activation of the TRY promoter by GL3 and TTG1, and TTG1 suppresses the activation of the CPC promoter by GL1 and GL3. Our data suggest that the transcriptional activation by the MBW complex involves alternative complex formation and that the two dimers can differentially regulate downstream genes.

One well-studied example for a single regulatory protein complex driving the evolution of multiple traits in plants is the R2R3MYB/basic helix-loop-helix (bHLH)/WD40 (MBW) complex (Broun, 2005; Koes et al., 2005; Ramsay and Glover, 2005; Serna and Martin, 2006; Feller et al., 2011). Together, the corresponding three genes are required for the regulation of metabolic pathways (anthocyanin and proanthocyanidin production) and the differentiation of epidermal cell types in higher plants (Broun, 2005; Koes et al., 2005; Ramsay and Glover, 2005; Serna and Martin, 2006; Feller et al., 2011). In Arabidopsis (*Arabidopsis thaliana*), this MBW complex has been implicated in five traits: anthocyanin and proanthocyanidin biosynthesis, seed coat mucilage production, and trichome and root hair patterning (Broun, 2005; Lepiniec et al., 2006; Balkunde et al., 2010; Tominaga-Wada et al., 2011). Trichome and root hair patterning traits are considered to be recent

evolutionary inventions, having evolved from the duplication and diversification of anthocyanin-controlling genes (Serna and Martin, 2006). In Arabidopsis, the WD40 protein is represented by the single-copy gene TRANSPARENT TESTA GLABRA1 (TTG1) that controls all five traits (Koornneef, 1981; Walker et al., 1999; Broun, 2005; Lepiniec et al., 2006; Balkunde et al., 2010; Tominaga-Wada et al., 2011). Three bHLH proteins regulate these five traits in a partially redundant manner, whereas the R2R3MYB factors regulate individual traits (Zhang et al., 2003; Broun, 2005; Lepiniec et al., 2006; Balkunde et al., 2010; Tominaga-Wada et al., 2011). The MBW proteins are considered to act together in a transcriptional activating complex in which both the R2R3MYB and the WD40 proteins bind to the bHLH protein. Higher ordered complexes are possible due to homodimerization or heterodimerization of bHLH proteins (Payne et al., 2000; Zhang et al., 2003; Feller et al., 2006).

The trichome pattern appears to be generated de novo (Hülskamp et al., 1994), that is, without preexisting information. By contrast, the root hair pattern is biased by positional cues from the underlying tissue layer such that root hairs are formed over the cleft of two underlying cortex cells (Berger et al., 1998). In both patterning systems, the MBW genes act in common to transcriptionally activate the homeobox transcription factor GLABRA2 (GL2) and other downstream genes. GL2 in turn promotes trichome and nonroot hair differentiation (Rerie et al.,

\* Address correspondence to martin.huelskamp@uni-koeln.de.

The author responsible for distribution of materials integral to the findings presented in this article in accordance with the policy described in the Instructions for Authors ([www.plantphysiol.org](http://www.plantphysiol.org)) is: Martin Hülskamp (martin.huelskamp@uni-koeln.de).

M.P., M.H., and J.F.U. designed the research; I.S., M.P., and K.K. performed the research; R.S., S.W.-P., J.F.U., M.K., and C.S.C. contributed new analytic tools and materials; S.W.-P., M.P., I.S., and K.K. analyzed the data; M.P. and M.H. wrote the article.

[www.plantphysiol.org/cgi/doi/10.1104/pp.15.00328](http://www.plantphysiol.org/cgi/doi/10.1104/pp.15.00328)

1994; Di Cristina et al., 1996; Masucci et al., 1996; Hung et al., 1998). Two bHLH genes, *GL3* and *ENHANCER OF GLABRA3 (EGL3)*, regulate trichome and root hair patterning in a partially redundant manner (Walker et al., 1999; Payne et al., 2000; Bernhardt et al., 2003). The R2R3MYB genes are represented by *GL1*, *MYB23*, and *WEREWOLF (WER)* (Oppenheimer et al., 1991; Lee and Schiefelbein, 1999; Kirik et al., 2001, 2005). *GL1* acts specifically in trichome patterning, *WER* in root hair patterning, and *MYB23* redundantly in both patterning processes. The intercellular communication is mediated by R3MYB transcription factors, including *CAPRICE (CPC)*, *TRIPTYCHON (TRY)*, *ENHANCER OF TRIPTYCHON AND CAPRICE1 (ETC1)*, *ETC2*, *ETC3*, *TRICHOMELESS1 (TCL1)*, and *TCL2* (Wada et al., 1997; Schellmann et al., 2002; Kirik et al., 2004a, 2004b; Simon et al., 2007; Wang et al., 2007; Wester et al., 2009; Gan et al., 2011). As judged by the phenotypic strength of their loss-of-function mutants, *TRY* and *CPC* are the major regulators during trichome development, and *CPC* is the most important R3MYB in root hair patterning. *TRY* and *CPC* are expressed in trichomes, and *CPC* is expressed in nonroot hair files, from where the respective proteins move into the neighboring cells (Schellmann et al., 2002; Wada et al., 2002) and repress the MBW functions. Movement was also reported for some of the MBW factors. In the root system, *GL3* was shown to be expressed in root hair files, from where it moves to the nonroot hair files (Bernhardt et al., 2005). In leaves, *TTG1* movement occurs from nontrichome cells to trichomes (Bouyer et al., 2008; Balkunde et al., 2011).

The MBW proteins are considered to act together in a trimeric transcriptional activating complex. This concept was initially derived from yeast two-hybrid data showing that *GL1* interacts with *GL3* and that *GL3* interacts with *TTG1* (Payne et al., 2000). Later studies confirmed the interactions between other MBW combinations (Bernhardt et al., 2003; Zhang et al., 2003; Baudry et al., 2004; Zimmermann et al., 2004; Tominaga et al., 2007). In support of this concept, coimmunoprecipitation experiments revealed an association of *TTG1* and *GL1* in vivo (Zhao et al., 2008). In addition, chromatin immunoprecipitation (ChIP) experiments demonstrated the presence of *GL1*, *GL3*, and *TTG1* at the *GL2*, *CPC*, and *ETC1* promoters (Morohashi et al., 2007; Zhao et al., 2008; Morohashi and Grotewold, 2009). Together, these data suggest the existence of a trimeric complex transcriptionally regulating downstream genes. Higher ordered complexes are possible due to homodimerization or heterodimerization of bHLH proteins (Payne et al., 2000; Zhang et al., 2003; Feller et al., 2006). The repression of the MBW function is thought to be governed by the binding of R3MYB proteins to *GL3/EGL3*, which in turn results in a replacement of *GL1/WER* in the trimeric complex, thereby rendering it inactive (Esch et al., 2003). The systematic analysis of *GL3* binding to target promoters in ChIP experiments revealed that *GL3* could bind to target promoters in three different manners (Morohashi et al.,

2007; Morohashi and Grotewold, 2009). First, binding to the *GL2*, *TTG2*, *CPC*, and *ETC3* promoters occurs only in the presence of *GL1*, suggesting that *GL1* is required for *GL3* recruitment to these promoters. Second, *GL3* binds to the *TRY* promoter independently of *GL1*. Third, *GL3* binds independently of *GL1* to the *GL3* promoter and negatively regulates its own expression without *GL1*. Together, these data suggest that the MBW factors may also act independently on some target promoters.

In this work, we show that MBW proteins involved in Arabidopsis trichome and root hair formation form alternatively bHLH/R2R3MYB or bHLH/WD40 dimers. We demonstrate by yeast three-hybrid assays, pulldown competition experiments, and fluorescence lifetime imaging microscopy (FLIM)-fluorescence resonance energy transfer (FRET) analysis that the formation of the two dimers is counteracted by the respective third protein. We further show that the activation of the *TRY* promoter by *GL3* and *TTG1* is counteracted by *GL1*. Conversely, the activation of the *CPC* promoter by *GL1* and *GL3* is inhibited by *TTG1*. Together, our data suggest that alternative dimers of MBW factors or their higher ordered multimers differentially regulate downstream genes.

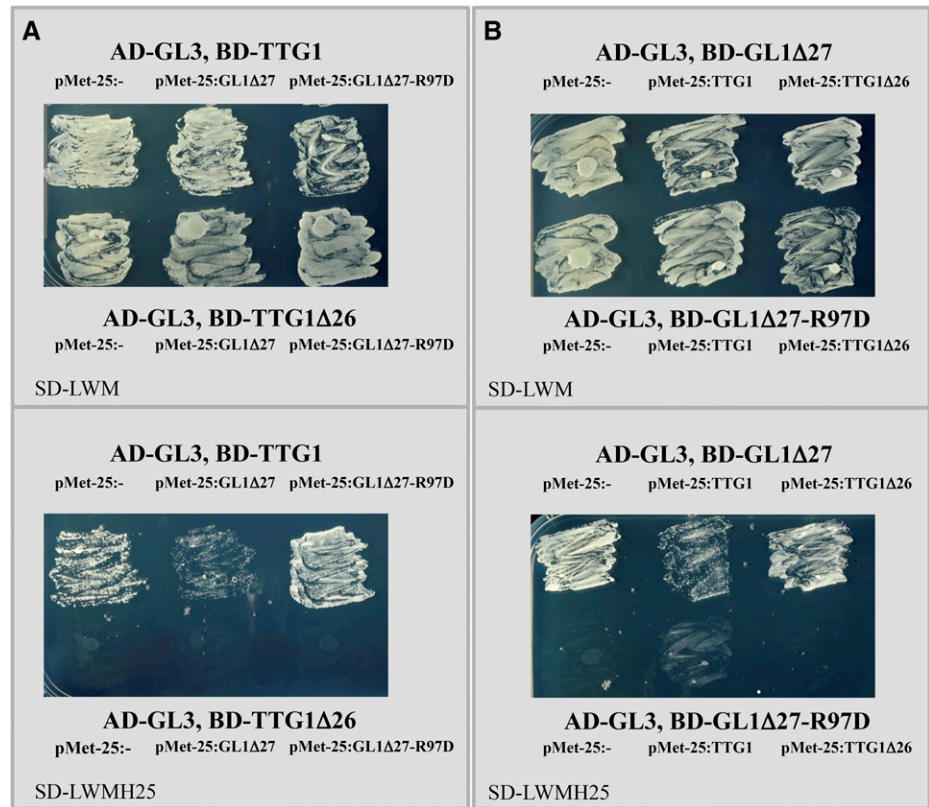
## RESULTS

### TTG1 Protein Interaction with GL3 Is Counteracted by GL1

The finding that *GL3* activates target genes with or without *GL1* (Morohashi et al., 2007; Morohashi and Grotewold, 2009) indicates that *GL3* does not need to form an MBW complex for transcriptional activation. This finding prompted us to analyze the formation of the MBW complex in more detail. We used the yeast three-hybrid system to analyze the *GL3*-*TTG1* interaction with and without *GL1*. Because full-length *GL1* is strongly autoactivating in yeast two-hybrid assays, we used a variant lacking the C-terminal 27 amino acids in all yeast (*Saccharomyces cerevisiae*) experiments (*GL1Δ27*; Supplemental Table S1; Payne et al., 2000). The *GL3*-*TTG1* interaction was monitored on plates lacking His, and *GL1Δ27* was additionally expressed under the control of a Met-repressible promoter. The *GL3*-*TTG1* interaction was clearly reduced when *GL1Δ27* was additionally expressed (Fig. 1A). The coexpression of a mutant version of *GL1* (*GL1Δ27-R97D*) that is impaired in its interaction with *GL3* (Supplemental Tables S1 and S2) had no effect on the *GL3*-*TTG1* interaction (Fig. 1A).

To study this in more detail, we performed a quantitative yeast three-hybrid analysis using  $\alpha$ -galactosidase as a reporter for the *GL3*-*TTG1* interaction. We found a strong reduction of the *GL3*-*TTG1* interaction by additionally expressed *GL1Δ27* but not a complete suppression (Fig. 2A). As negative controls, we included *GL1* and *TTG1* protein mutants showing strongly reduced interactions with *GL3* (*GL1Δ27-R97D* and *TTG1Δ26*; Fig. 2; Supplemental Tables S1 and S2).

**Figure 1.** Qualitative yeast three-hybrid assays for protein interactions of GL1, GL3, and TTG1. A, The interaction between GL3 and TTG1 was analyzed using fusions with the GAL4 activation domain (AD-GL3) and the binding domain (BD-TTG1). BD-TTG1Δ26 was used as a negative control. The vector immanent rest protein of 62 amino acids (-), GL1Δ27, and GL1Δ27-R97D were expressed as free proteins under the control of the Met-repressible pMet-25 promoter. Growth was compared after 2 d on synthetic dropout selection medium (SD-LWM) or synthetic dropout interaction medium containing 25 mM 3-aminotriazole (SD-LWMH25). B, The GL1-GL3 interaction was studied using AD-GL3 and BD-GL1Δ27 with GL1Δ27-R97D as a negative control. The vector immanent rest protein of 62 amino acids (-), TTG1, and TTG1Δ26 were expressed as free proteins under the control of the Met-repressible pMet-25 promoter under the same selection scheme as in A.



We confirmed this interference of GL1 with the GL3-TTG1 interaction using the luminescence-based mammalian interactome (LUMIER) assay (Barrios-Rodiles et al., 2005): protein fusions to either Protein A (ProtA) or *Renilla reniformis* luciferase were expressed in human HEK293TN cells. The ProtA-tagged protein was immunoprecipitated with IgG beads, and the amounts of coimmunoprecipitated proteins were quantified in a luciferase assay. The pull-down ratio of TTG1 GL3 was defined as 100%. The addition of free GL1, but not the mutated GL1-R97D (Supplemental Tables S1 and S2), caused a reduced pull-down efficiency of luciferase-tagged GL3 (Table I).

We also tested whether the addition of the R2R3MYB protein WER can inhibit the GL3-TTG1 interaction. In yeast three-hybrid experiments and in LUMIER assays, WER inhibited the GL3-TTG1 interaction, indicating that GL1 and WER show the same interaction behavior (Tables I and II). Coexpression of TRY and CPC had no effect on the GL3-TTG1 interaction, ruling out the possibility that their inhibitory effect on GL3 TTG1 is caused by preventing their interaction (Table II).

#### GL1 Interaction with GL3 Is Counteracted by TTG1

In the next step, we tested whether the GL3-GL1 interaction also can be inhibited by TTG1. In yeast three-hybrid assays, the GL3-GL1Δ27 interaction was analyzed with and without coexpressed TTG1. We

found reduced interaction of GL3 with GL1Δ27 in the presence of TTG1 (Fig. 1B). As a negative control, we used TTG1Δ26 (Fig. 1B; Supplemental Table S1). The expression of TTG1Δ26 did not interfere with the GL3-GL1Δ27 interaction. Quantitative yeast three-hybrid analysis revealed an 8-fold reduced  $\alpha$ -galactosidase activity when TTG1 was additionally expressed (Fig. 2B). TTG1Δ26 did not affect the interaction (Fig. 2B).

In order to test whether the inhibition of the GL3-GL1Δ27 interaction depends on the concentration of TTG1, we tested the competitive effect of varying TTG1 expression levels in the yeast three-hybrid assay. TTG1 expression levels were regulated by varying the Met concentration. Without Met (highest TTG1 levels), no GL3-GL1Δ27 interaction was detected; successively stronger reporter activity was found at increasing Met levels, suggesting a dosage-dependent inhibition of the GL3-GL1Δ27 interaction by TTG1 (Fig. 3, A and B). We confirmed this concentration-dependent interference of TTG1 with the GL1-GL3 interaction using the LUMIER assay. When adding increasing amounts of untagged TTG1, the amount of coprecipitated luciferase-GL3 dropped successively (Fig. 3C). As a negative control, we used the TTG1Δ26 variant that showed no interaction with GL3 in the LUMIER assay (Fig. 3D; Supplemental Table S2). This mutant version did not interfere with the GL3-GL1 interaction (Fig. 3C).

Together, these data suggest that two alternative dimeric complexes, GL3 TTG1 and GL1 GL3, are formed and that the formation of each can be counteracted by the respective third protein.

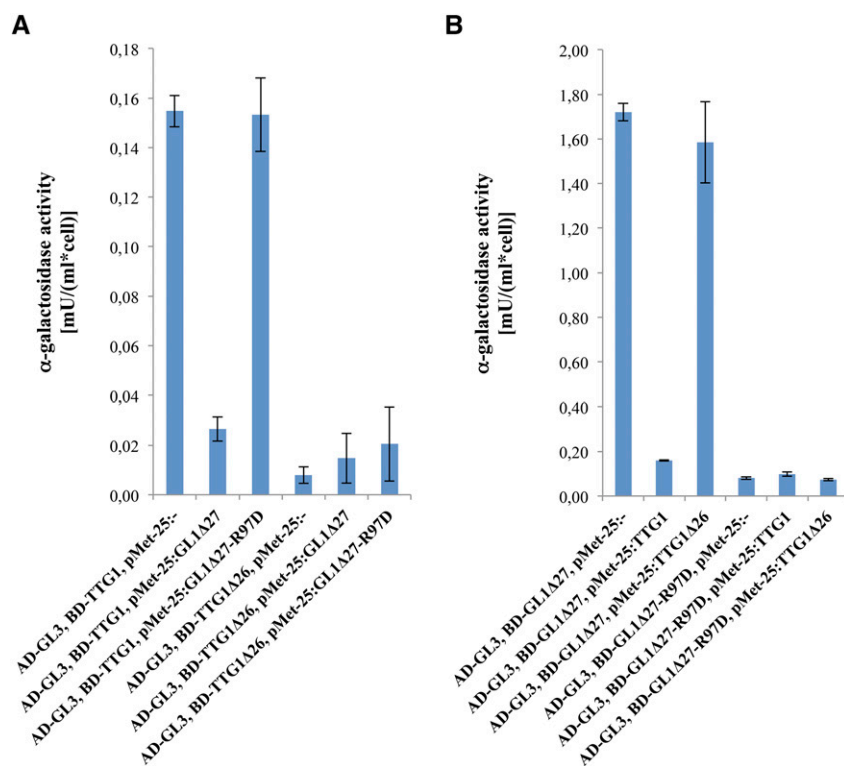


**Figure 2.** Quantitative yeast three-hybrid assays of the competitive binding of GL1 and TTG1 to GL3. Quantitative analysis of interactions by  $\alpha$ -galactosidase assays is shown. Means and SD are shown for three replicates. Cells were grown in synthetic dropout selection medium and analyzed after 16 h of growth by the *p*-nitrophenyl- $\beta$ -D-glucopyranoside assay. A, Repression of the AD-GL3 and BD-TTG1/BD-TTG1 $\Delta$ 26 interactions by GL1. AD-GL3, BD-TTG1, or BD-TTG1 $\Delta$ 26 was coexpressed with GL1 $\Delta$ 27 or GL1 $\Delta$ 27-R97D under the control of the Met-repressible pMet-25 promoter. B, Repression of the AD-GL3 and BD-GL1 $\Delta$ 27/BD-GL1 $\Delta$ 27-R97D interactions by TTG1. AD-GL3, BD-GL1 $\Delta$ 27, or BD-GL1 $\Delta$ 27-R97D was coexpressed with TTG1 or TTG1 $\Delta$ 26 under the control of the Met-repressible pMet-25 promoter.

### FLIM-FRET Reveals Competition in Vivo

To study the MBW complex formation of GL1, GL3, and TTG1 in vivo, we performed a FLIM-based FRET analysis. With this method, the interaction of fluorescent protein-tagged proteins can be monitored by FRET, which, in turn, is measured by a shortened fluorescence lifetime of the donor protein (here cyan fluorescent protein [CFP]). Toward this end, CFP-GL1 alone and in combination with yellow fluorescent protein (YFP)-GL3 or with YFP-GL3 and TTG1 were transiently expressed and analyzed in tobacco (*Nicotiana tabacum*) leaf epidermal cells. Coexpression of CFP-GL1 with YFP-GL3 caused a clear shift to a shorter fluorescence lifetime of CFP-GL1 to  $2.59 \pm 0.12$  ns compared with  $2.95 \pm 0.09$  ns when CFP-GL1 is expressed without any other protein (Fig. 4, A and B; Supplemental Fig. S1). This indicates that FRET occurred between CFP-GL1 and YFP-GL3. The additional expression of TTG1 results in a fluorescence lifetime of  $2.7 \pm 0.16$  ns, which is significantly longer than the lifetime of CFP-GL1 coexpressed with YFP-GL3 (Fig. 4, A and B; Table III). Thus, the interaction of CFP-GL1 and YFP-GL3 is counteracted by TTG1 in vivo as well.

In the course of our experiments, we noticed that YFP-GL3 was typically found in both the nucleoplasm and speckles (Fig. 4E). As speckle formation was previously described to be dependent on GL1 and TTG1 (Zhao et al., 2008), we extended our analysis by separately considering the nucleoplasm and the speckles. In the nucleoplasm, the shift to a prolonged lifetime could be observed as in the whole nucleus, indicating that

TTG1 interferes with the interaction of CFP-GL1 and YFP-GL3 (Fig. 4, A and C). In speckles, the distribution of CFP-GL1 lifetime showed a main peak and a clear shoulder (Fig. 4D). This curve can be clearly separated using a two-peak Gaussian fit analysis in one big peak with a shorter lifetime and a second but smaller peak with longer lifetime (Fig. 4F). These data suggest the presence of two CFP-GL1 populations. A small population shows an increased lifetime of CFP-GL1 of 2.91 ns, which can be interpreted as a strongly reduced interaction of CFP-GL1 with YFP-GL3 due to the presence of TTG1. A larger fraction exhibits a decreased lifetime of 2.58 ns, suggesting a not affected interaction of CFP-GL1 and YFP-GL3. These findings might indicate that, also in vivo at least in nuclear speckles, two types of complexes, CFP-GL1 and YFP-GL3 as well as CFP-GL1

**Table 1.** Pulldown of different TTG1-bHLH-MYB complexes with ProtA fused to TTG1, Luciferase fused to the bHLH factor, and untagged MYB factors using the LUMIER technology

The pulldown ratios (percentage pulldown of input) were normalized to the combination TTG1 and GL3 without additional MYB proteins.

ProtA Fusion	Luciferase Fusion	Free Protein	Pulldown Ratio
TTG1	GL3	GL1	$71.1 \pm 5.3$
TTG1	GL3	WER	$70.4 \pm 1.3$
TTG1	GL3	TRY	$109.7 \pm 2.5$
TTG1	GL3	CPC	$101.7 \pm 3.6$
TTG1	GL3	GL1-R97D	$95.5 \pm 5.5$
TTG1	GL3		$100.0 \pm 3.7$

**Table II.** Yeast three-hybrid interaction studies to study interference with the *TTG1-GL3* interaction

Transformed yeast colonies were incubated at 30°C on different media as indicated. Colony growth was determined after 2 d. AD, GAL4 activation domain; BD, GAL4 DNA binding domain; LWA, synthetic dropout medium lacking Leu, Trp, and adenine; LWAH10, synthetic dropout medium lacking Leu, Trp, adenine, and His with 10 mM 3-aminotriazole to test the interactions. +, Growth; –, no growth.

BD	AD	Free Protein	LWA	LWAH10
TTG1	GL3	GL1Δ27	+	–
TTG1	GL3	GL1Δ27-R97D	+	+
TTG1	GL3	WER	+	–
TTG1	GL3	TRY	+	+
TTG1	GL3	CPC	+	+
TTG1	GL3		+	+

and *TTG1*, exist side by side. We presumably could not resolve these complexes within the nucleoplasm due to higher mobility and a weaker degree of clustering there, resulting in an intermediate fluorescence lifetime value representing a mixture of complexes.

#### The Activation of the *TRY* Promoter by *GL3* and *TTG1* Is Counteracted by *GL1*

The competition behavior of the *GL1*, *GL3*, and *TTG1* proteins raises the question of whether the competition also occurs at the level of target promoter activation. We aimed to analyze this using conditions that minimize endogenous transcriptional feedback loops and the overall complexity of the system. Toward this end, we expressed the three MBW proteins under the control of the 35S promoter along with minimal promoter fragments of two target promoters, *TRY* and *CPC*, in *Arabidopsis* suspension cultures. Although we found background expression of *GL1*, *GL3*, *TTG1*, and some of the homologs with partially redundant functions (*MYB23*, *WER*, and *EGL3*) in the suspension culture cells (Supplemental Fig. S2), the two target promoters were inactive without additionally expressed MBW proteins (Tables IV–VII). The analysis of the *TRY* and *CPC* promoter activation by single MBW proteins suggests that the *TTG1* and R2R3MYB background levels can contribute to the promoter activation (Tables IV–VII). Therefore, we considered the three MBW proteins to be present in all experiments and focused on the question of whether extra expression of one protein can counteract the activation of the promoters by the two other proteins.

For *TRY*, we used a 620-bp promoter fragment shown to be sufficient to mediate the correct transcriptional regulation in leaves and trichomes and to fully rescue the trichome phenotype (Pesch and Hülskamp, 2011). As expected, *pTRY:GUS* was strongly activated upon coexpression of *GL3*, *GL1*, and *TTG1* (Table IV). This value was defined as 100% in each experiment to enable a comparison of the different experiments. Strikingly, the activation of *pTRY:GUS* was higher without coexpressed

*GL1*, suggesting that *GL1* counteracts the transcriptional activation by *GL3* and *TTG1*. When using *GL1-R97D*, we found no influence on the *TRY* promoter activation by *GL3* and *TTG1* (Table IV). The coexpression of *TTG1Δ26* (Supplemental Table S1) with *GL3* could not trigger the promoter activation as seen with the *GL3 TTG1* combination, suggesting that the *TTG1-GL3* interaction is relevant for the activation of the *TRY* promoter (Table IV).

In all current models, *TRY/CPC* is considered to inhibit the activation of the trimeric complex by replacing *GL1*, and the absence of *GL1* renders the MBW complex inactive. The finding that *GL1* acts as a negative regulator of the *GL3 TTG1*-dependent activation of the *TRY* promoter raises the question of whether *TRY/CPC* can repress the *GL3 TTG1*-dependent *pTRY* activation. Our assays showed that *TRY* or *CPC* effectively suppresses the activation by *GL1/GL3/TTG1* as well as by *GL3/TTG1* (Table V). This suggests that *TRY* and *CPC* can exert their repression by rendering *GL3 TTG1* inactive.

#### The Activation of the *CPC* Promoter by *GL3* and *GL1* Is Repressed by *TTG1*

The unexpected regulation scheme found for the *TRY* promoter prompted us to compare it with that for the *CPC* promoter. For the analysis of the activation of the *CPC* promoter by *GL3*, *GL1*, and *TTG1*, we used a 525-bp-long 5' upstream region previously shown to drive correct expression in roots and leaves and to rescue the trichome phenotype (Pesch and Hülskamp, 2011). The addition of *GL1*, *GL3*, and *TTG1* resulted in a strong enhancement (defined as 100%). In contrast to the *TRY* promoter, *TTG1* counteracted the activation of the *CPC* promoter by *GL3* and *GL1* (Table VI). The binding of *TTG1* to *GL3* is relevant for the repression of *CPC* promoter activation by *GL1* and *GL3* because *TTG1Δ26* could not counteract *GL1 GL3* (Table VI). The interaction of *GL1* with *GL3* is necessary, as the addition of *GL1-R97D* did not lead to an increased *CPC* activation (Table VI). As observed for the *TRY* promoter, we detected efficient repression by *TRY* and *CPC* (Table VII).

## DISCUSSION

In this article, we report that *GL1* and *TTG1* show competitive binding to *GL3* rather than a simultaneous binding of both proteins to *GL3*, as suggested before. The competition efficiency differed between the experimental setups, such that binding of *TTG1* to *GL3* was only partially affected by *GL1/WER* in pulldown experiments and almost abolished in yeast three-hybrid experiments. There are many explanations for this, including different concentration ratios of the respective proteins, the influence of different tags, and the molecular kinetics of the detection systems. Therefore, it is not possible to make conclusions on the stoichiometry of the interactions and competitions. However, three observations suggest that the competition



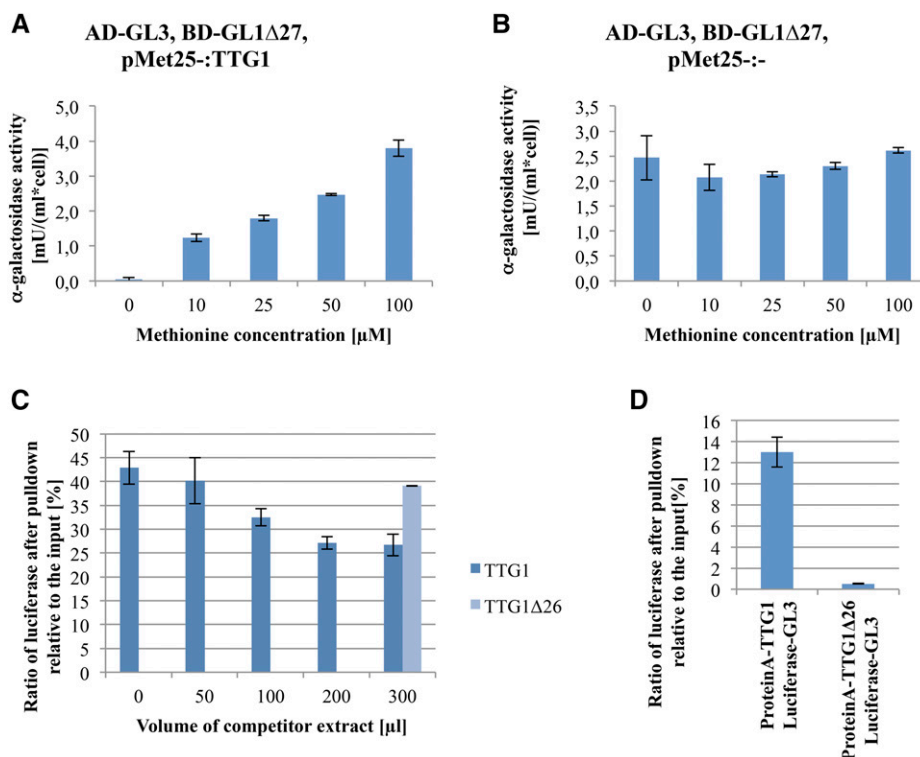


**Figure 3.** Dosage-dependent inhibition of the GL1-GL3 interaction by TTG1. A and B, Yeast three-hybrid assay. GL3 N terminus fused to the GAL4 transcriptional activation domain (AD-GL3) was coexpressed with GL1Δ27 N terminus fused to the GAL4 DNA binding domain (BD-GL1Δ27) in yeast. TTG1 (A) or the empty vector (B) was expressed under the control of the Met-repressible pMet-25 promoter. The  $\alpha$ -galactosidase activity was determined in three replicates at different Met concentrations (0, 10, 25, 50, and 100  $\mu$ M). The highest concentration of TTG1 (without Met) causes a complete repression of GL3-GL1Δ27 interaction, and lower levels of TTG1 result in higher interaction levels ( $P < 10^{-4}$ , Student's *t* test). No significant differences were observed when using the empty vector instead of TTG1 ( $P > 0.2$ , Student's *t* test). C and D, Pull-down assays by LUMIER. Proteins were expressed separately in human cell culture (HEK293TN): GL3 as an N-terminal fusion to the *R. reniformis* luciferase; GL1, TTG1, and TTG1Δ26 as N-terminal fusions to the *Staphylococcus aureus* ProtA; and TTG1 and TTG1Δ26 and the corresponding empty vector control without any tag. Different proteins were combined after cell lysis, and Luciferase was measured after pulldown of the ProtA-fused proteins. C, Luciferase-GL3 and ProtA-GL1 combined with different concentrations of TTG1 or TTG1Δ26 (without any tag). D, To test the protein interaction properties of TTG1 and TTG1Δ26 with GL3, Luciferase-GL3 was mixed with either ProtA-TTG1 or ProtA-TTG1Δ26. Each experiment was performed in three replicates, and SD values are shown as error bars for each column. The pulldown rates of GL3 by GL1 dropped significantly upon the addition of TTG1 but not by TTG1Δ26, indicating that TTG1 interferes with the GL3-GL1 interaction.

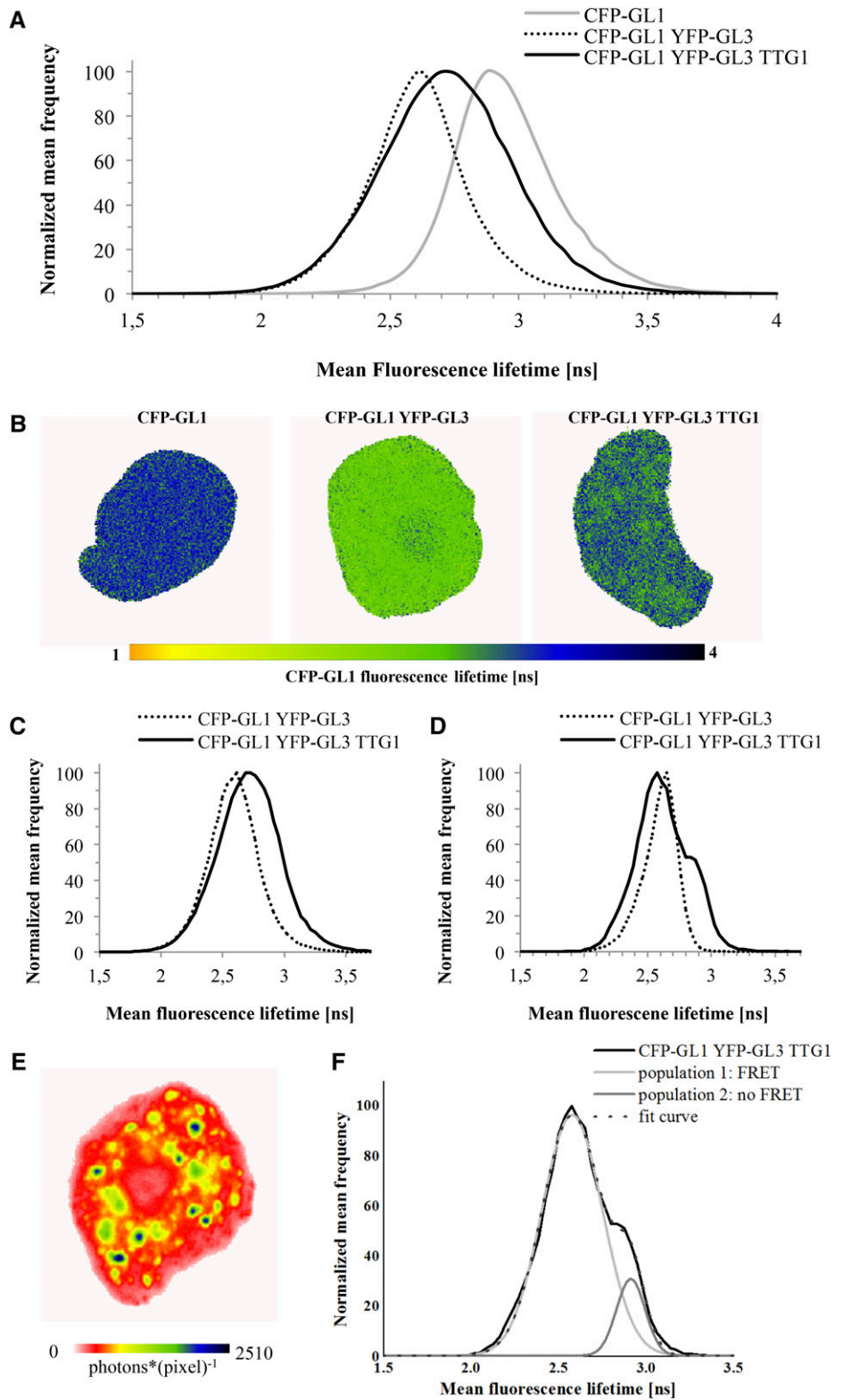
takes place within a reasonable range of biologically meaningful concentration ratios. First, the competition is seen when the respective genes are expressed under the control of the same promoters. Second, the interaction of GL1 and TTG1 with GL3 can be inhibited by additional expression of TTG1 and GL1, respectively. This renders it unlikely that posttranscriptional or posttranslational regulation of one component creates artificially large differences in the concentration ratios. In addition, our pulldown and yeast three-hybrid data clearly show that the competition becomes more efficient with increasing levels of the competing protein, indicating that the competition occurs in a dosage-dependent manner.

#### bHLH Proteins Can Form Two Mechanistically Different Types of Alternative Complexes

Our finding that GL1/WER can counteract the GL3-TTG1 interaction and that TTG1 can counteract the

GL1-GL3 interaction suggests that the R2R3MYB and TTG1 proteins compete for binding to GL3 and that two alternative complexes are formed (Fig. 5A). This raises the question of how this type of competitiveness is related to the competition of R2R3MYBs and R3MYBs for binding to bHLH proteins (Esch et al., 2003; Tominaga et al., 2008; Wester et al., 2009). If the competition between R2R3MYB and R3MYB for binding to bHLH proteins is mechanistically related to the R2R3MYB/TTG1 competition for binding to bHLH proteins, one would expect that R3MYBs can also interfere with the TTG1-GL3 interaction. We found no effect of TRY or CPC on the GL3-TTG1 interaction in pulldown and yeast three-hybrid experiments. These data suggest that GL3 is involved in two mechanistically distinct types of competitive complex formation: first, the competitive binding of GL1 and TTG1 to GL3; and second, the competitive binding of GL1 and TRY/CPC to GL3. The latter is thought to be the molecular

**Figure 4.** FLIM-FRET analysis of the CFP-GL1, YFP-GL3, and TTG1 interactions in tobacco cells. A, Normalized mean frequency of the CFP-GL1 fluorescence lifetime per pixel was measured for CFP-GL1 alone ( $n = 10$ ), for CFP-GL1 coexpressed with YFP-GL3 ( $n = 22$ ), and for CFP-GL1 and YFP-GL3 coexpressed with TTG1 ( $n = 34$ ). B, CFP-GL1 fluorescence lifetime in selected tobacco nuclei in different combinations as indicated. C to F, CFP-GL1 fluorescence lifetime in the nucleoplasm and speckles. C, Nucleoplasm. D, Nuclear speckles. E, Distribution of nuclear speckles as indicated by CFP-GL1 fluorescence intensity. F, Fluorescence lifetime of CFP-GL1 in speckles of CFP-GL1, YFP-GL3, and TTG1 coexpressing cells. Note the shoulder on the right side.



basis for the repressor function of the R3MYBs, such that the removal of GL1 from the MBW complex renders the complex inactive (Esch et al., 2003; Tominaga et al., 2008; Wester et al., 2009). How can this model be adopted to the alternative GL3 TTG1 and GL1 GL3

complex scenario? The removal of GL1 from the GL1 GL3 complex by TRY/CPC binding to GL3 can easily explain how they repress the CPC promoter. The repression of the TRY promoter, however, requires an alternative explanation, as GL1 acts as a negative

**Table III.** Normalized mean fluorescence lifetime of CFP-GL1 alone and in combination with YFP-GL3 or YFP-GL3 and TTG1 in nuclei of tobacco leaf epidermal cells

Parameter	Coexpressed Construct		
	CFP-GL1	CFP-GL1 YFP-GL3 <sup>a</sup>	CFP-GL1 YFP-GL3 TTG1 <sup>b</sup>
Normalized mean fluorescence lifetime <sup>c</sup>	1.00 ± 0.03	0.87 ± 0.05	0.92 ± 0.05
No. of measured cells	16	41	40

<sup>a</sup>Statistical significance of the fluorescence lifetime of CFP-GL1 compared with CFP-GL1 YFP-GL3 expressing cells:  $P < 10^{-13}$  (Student's *t* test). <sup>b</sup>Statistical significance of the fluorescence lifetime of CFP-GL1 YFP-GL3 compared with CFP-GL1 YFP-GL3 TTG1 expressing cells:  $P < 0.0002$  (Student's *t* test). <sup>c</sup>Data show the means ± SD normalized to the fluorescence lifetime of CFP-GL1 alone.

regulator here. It is conceivable that, in this context, CPC/TRY can render the GL3 TTG1 complex inactive. Thus, TRY and CPC may exert their inhibitory function by the removal of GL1 from GL3 and/or by directly inhibiting GL3 (Fig. 5A).

#### Is the Formation of Alternative MBW Protein Complexes in Conflict with Previous Biochemical Data?

Initially, the concept of a trimeric MBW complex was derived from pairwise yeast two-hybrid data showing that GL1 and TTG1 can bind to GL3 and that GL1 and TTG1 cannot interact directly (Payne et al., 2000). Later, coimmunoprecipitation experiments of Arabidopsis protein extracts revealed an association of TTG1 and GL3 as well as an association of TTG1 and GL1 (Zhao et al., 2008). ChIP experiments confirmed

the simultaneous presence of GL1 and TTG1 at several target promoters (Zhao et al., 2008; Morohashi and Grotewold, 2009). These data suggest that the three proteins can associate in vivo. However, they can easily be explained without challenging our conclusion that differential complex formation occurs. (1) As bHLH proteins can homodimerize or heterodimerize (Payne et al., 2000; Zhang et al., 2003; Feller et al., 2006), it is possible that biochemical studies detect all three proteins because they are connected through the bHLH-bHLH interactions (Fig. 5B). (2) MBW complexes could be stabilized by other transcriptional cofactors in planta.

There are also data that challenge the previous concepts and support our findings. First, the transformation of Arabidopsis protoplasts with GL1 and GL3 was sufficient to trigger CPC expression (Wang et al., 2008). Second, ChIP revealed that GL3 binding to promoter regions may or may not require GL1 in a

**Table IV.** Cotransformation promoter activation assay in Arabidopsis cell suspension culture using pTRY:GUS and different combinations of the effectors GL1, GL3, and TTG1 under the control of the cauliflower mosaic virus (CaMV) 35S promoter

As the transformation efficiencies vary between experiments done at different time points, we provide data from the experiments using the mutated GL1 and TTG1 proteins as separate experimental sets. Each data point is the mean of three biological replicates. Dashes indicate the addition of the CaMV 35S effector construct without any coding sequence (CDS) to ensure the comparability of the *Agrobacterium tumefaciens* amount.

35S:CDS			Absolute Activity of pTRY:GUS	Relative Activity Normalized to the Combination GL1, GL3, and TTG1
			pmol mg <sup>-1</sup> protein min <sup>-1</sup>	%
Set A				
GL1	GL3	TTG1	185.0 ± 33.6	100.0
-	GL3	TTG1	424.8 ± 34.3	229.6
GL1	GL3	-	171.6 ± 15.9	92.8
GL1	-	TTG1	-4.4 ± 1.7	-2.4
GL1	-	-	-2.2 ± 0.9	-1.2
-	GL3	-	286.9 ± 21.6	155.0
-	-	TTG1	-2.4 ± 2.7	1.3
-	-	-	-5.1 ± 3.3	-2.8
Set B				
GL1	GL3	TTG1	296.5 ± 55.7	100.0
GL1	GL3	TTG1Δ26	239.5 ± 11.0	80.8
GL1	GL3	-	262.1 ± 21.8	88.4
-	GL3	TTG1	1,080.0 ± 28.8	364.2
-	GL3	TTG1Δ26	424.8 ± 46.5	143.2
-	GL3	-	607.7 ± 158.7	204.9
-	-	-	11.6 ± 0.8	3.9
Set C				
GL1	GL3	TTG1	173.8 ± 23.8	100.0
-	GL3	TTG1	309.3 ± 26.0	178.0
GL1-R97D	GL3	TTG1	385.2 ± 18.7	221.6
-	-	-	3.8 ± 0.3	2.2



**Table V.** Cotransformation promoter activation assay in *Arabidopsis* cell suspension culture using *pTRY:GUS* and different combinations of the effectors *GL1*, *GL3*, *TTG1*, *TRY*, and *CPC* under the control of the *CaMV 35S* promoter as indicated

The results represent means of three samples. The whole experiment was performed two times independently. Dashes indicate the addition of the *CaMV 35S* effector construct without any CDS.

35S:CDS				Absolute Activity of <i>pTRY:GUS</i>	Relative Activity Normalized to the Combination <i>GL1</i> , <i>GL3</i> , and <i>TTG1</i>
				<i>pmol mg<sup>-1</sup> protein min<sup>-1</sup></i>	%
<i>GL1</i>	<i>GL3</i>	<i>TTG1</i>	–	275.2 ± 14.0	100.0
<i>GL1</i>	<i>GL3</i>	<i>TTG1</i>	<i>TRY</i>	52.7 ± 6.6	19.1
<i>GL1</i>	<i>GL3</i>	<i>TTG1</i>	<i>CPC</i>	40.3 ± 14.4	14.6
–	<i>GL3</i>	<i>TTG1</i>	–	580.0 ± 56.1	210.7
–	<i>GL3</i>	<i>TTG1</i>	<i>TRY</i>	110.1 ± 21.3	40.0
–	<i>GL3</i>	<i>TTG1</i>	<i>CPC</i>	49.3 ± 24.2	17.9
–	–	–	–	16.3 ± 1.8	5.9

promoter-specific manner (Morohashi et al., 2007; Morohashi and Grotewold, 2009). Thus, the picture emerging is that the regulation of target promoters by the MBW complex involves differential complex formation of R2R3MYB *GL3* and *TTG1* *GL3* dimers or higher order complexes caused by homodimerization or heterodimerization of bHLH proteins or other proteins (Fig. 5B). The existence of higher ordered MBW complexes containing additional proteins is suggested by the recent finding that the WRKY transcription factor *TTG2* can bind directly to *TTG1* and through *TTG1* to *GL3* (Pesch et al., 2014). This interaction scheme seems to be relevant, as *TTG2* regulates the *TRY* promoter by enhancing the transcriptional activation by the MBW complex (Pesch et al., 2014).

### Differential Regulation of Target Promoters by Alternative MBW Protein Complexes

The in vivo analysis of the role of transcription factors in the regulation of specific target promoters is limited. This is particularly true for gene regulatory networks, where it is typically not possible to decide whether transcriptional changes of target genes in different mutant backgrounds reflect direct regulation events or indirect effects through the upstream gene regulatory network. To reduce the complexity, we studied small functional promoter fragments of *TRY* and *CPC* in cell types in which they are not activated. Our data suggest different regulation schemes for the two promoters. The activation of the *TRY* promoter by

**Table VI.** Cotransformation promoter activation assay in *Arabidopsis* cell suspension culture using *pCPC:GUS* and different combinations of the effectors *GL1*, *GL3*, and *TTG1* under the control of the *CaMV 35S* promoter

As the transformation efficiencies vary between experiments done at different time points, we provide data from the experiments using the mutated *GL1* and *TTG1* proteins as separate experimental sets. Each data point is the mean of three biological replicates. Dashes indicate the addition of the *CaMV 35S* effector construct without any CDS to ensure the comparability of the *A. tumefaciens* amount.

35S:CDS				Absolute Activity of <i>pCPC:GUS</i>	Relative Activity Normalized to the Combination <i>GL1</i> , <i>GL3</i> , and <i>TTG1</i>
				<i>pmol mg<sup>-1</sup> protein min<sup>-1</sup></i>	%
Set A					
<i>GL1</i>	<i>GL3</i>	<i>TTG1</i>		302.1 ± 46.4	100.0
<i>GL1</i>	<i>GL3</i>	–		919.7 ± 94.6	304.4
<i>GL1</i>	–	<i>TTG1</i>		2.5 ± 0.8	0.8
–	<i>GL3</i>	<i>TTG1</i>		127.5 ± 12.7	42.2
<i>GL1</i>	–	–		5.4 ± 3.4	1.8
–	<i>GL3</i>	–		66.8 ± 0.4	22.1
–	–	<i>TTG1</i>		3.1 ± 2.7	1.0
–	–	–		2.8 ± 0.3	0.9
Set B					
<i>GL1</i>	<i>GL3</i>	<i>TTG1</i>		545.1 ± 66.5	100.0
<i>GL1</i>	<i>GL3</i>	–		1,766.9 ± 222.8	324.1
<i>GL1</i>	<i>GL3</i>	<i>TTG1Δ26</i>		1,832.2 ± 205.1	336.1
–	–	–		3.8 ± 0.7	0.7
Set C					
<i>GL1</i>	<i>GL3</i>	<i>TTG1</i>		388.9 ± 99.3	100.0
<i>GL1-R97D</i>	<i>GL3</i>	<i>TTG1</i>		218.0 ± 53.6	56.1
–	<i>GL3</i>	<i>TTG1</i>		158.4 ± 81.5	40.7
–	<i>GL3</i>	–		83.3 ± 12.0	21.4
<i>GL1-R97D</i>	<i>GL3</i>	–		107.0 ± 35.2	27.5
<i>GL1</i>	<i>GL3</i>	–		1,608.6 ± 345.9	413.6
–	–	–		4.7 ± 0.5	1.2

**Table VII.** Cotransformation promoter activation assay in *Arabidopsis* cell suspension culture using *pCPC:GUS* and different combinations of the effectors GL1, GL3, TTG1, TRY, and CPC under the control of the *CaMV 35S* promoter as indicated

Results represent means of three samples. The whole experiment was performed two times independently. Dashes indicate the addition of the *CaMV 35S* effector construct without any CDS.

35S:CDS				Absolute Activity of <i>pCPC:GUS</i>	Relative Activity Normalized to the Combination GL1, GL3, and TTG1
				$\text{pmol mg}^{-1} \text{ protein min}^{-1}$	%
GL1	GL3	TTG1	–	407.3 ± 78.2	100.0
GL1	GL3	TTG1	TRY	65.9 ± 2.3	16.2
GL1	GL3	TTG1	CPC	65.7 ± 12.1	16.1
GL1	GL3	–	–	1,666.0 ± 467.5	409.0
GL1	GL3	–	TRY	177.0 ± 33.0	43.5
GL1	GL3	–	CPC	270.0 ± 16.3	66.3
–	–	–	–	9.2 ± 2.4	2.3

GL3 and TTG1 is suppressed by GL1. Conversely, TTG1 represses the activation of the *CPC* promoter by GL1 and GL3. When taking the formation of alternative MBW complexes into account, the simplest interpretation of these regulation schemes is that the *TRY* promoter is activated by GL3 TTG1 and that the *CPC* promoter is activated by GL1 GL3. The GL1 protein might counteract the formation of the GL3 TTG1 dimer, or TTG1 the GL1 GL3 dimer, and thereby the activation of the *TRY* or *CPC* promoter, respectively.

Our findings appear to contradict previous results. In the case of *TRY*, it was previously shown that the expression of *TRY* is absent in *gl1* mutants (Digiuni et al., 2008) and that GL1 associates with the *TRY* promoter in ChIP experiments but is not necessary for GL3 binding (Morohashi et al., 2007; Morohashi and Grotewold, 2009). Under the assumption that our promoter assays reflect the basal reaction scheme of the MBW proteins, the discrepancies could be explained by the above-mentioned network complexity: the absence of *TRY* expression in the *gl1* mutant could be explained

by expression changes of other genes in the regulatory network that, in turn, have an effect on *TRY* expression. A possible explanation for the association of GL1 to the *TRY* promoter in ChIP experiments is that this represents the situation in the nontrichome cells, where the *TRY* promoter is shut off. As whole leaves are used for ChIP experiments, it is not possible to capture spatial differences. Our reaction schemes for the *CPC* promoter are largely in agreement with other data. In ChIP experiments, GL3 and GL1 bind to the *CPC* promoter simultaneously, and the transcriptional activation through induced GL3 expression requires the presence of GL1 (Morohashi et al., 2007; Zhao et al., 2008; Morohashi and Grotewold, 2009).

#### Consequences of Alternative Complex Formation for Patterning Models

If the MBW complex is not represented by a single trimeric complex but by two alternative dimers that

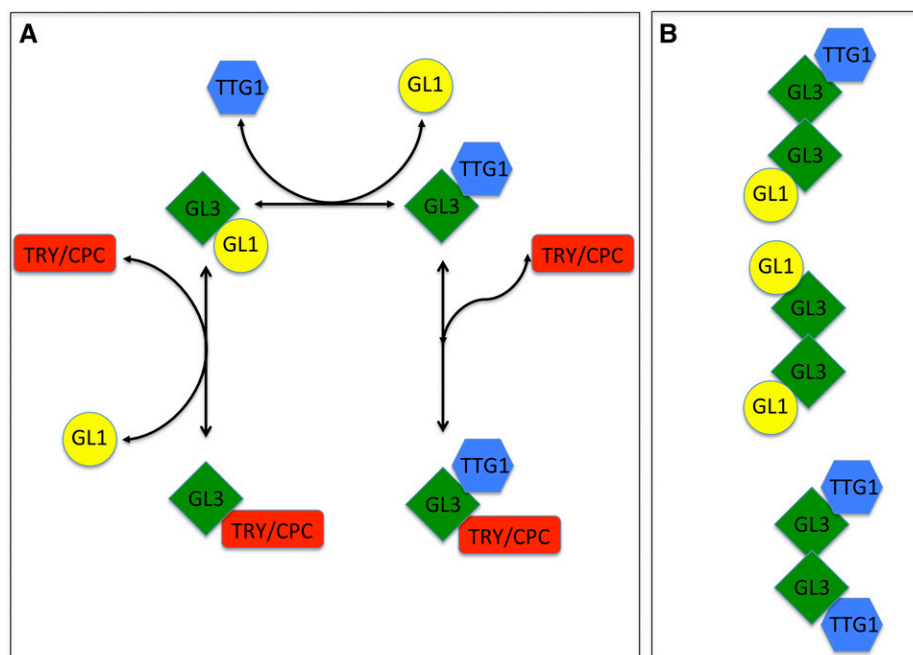


**Figure 5.** Model depicting possible alternative protein complexes of the MBW proteins and their inhibitors. A, The formation of two alternative GL1 GL3 and GL3 TTG1 dimers and the respective interaction scheme with the R3 MYBs TRY and CPC. B, As GL3 can homodimerize, it is likely that higher ordered complexes are formed. Examples of positive complexes combining dimers are shown in A. Additional combinations with the R3MYBs are possible.

regulate different downstream genes, the regulatory complexity that controls trichome and root hair patterning increases drastically. One might expect that different promoters become activated depending on the relative concentrations of the three MBW proteins, which in turn leads to different ratios of GL1 GL3 and GL3 TTG1 dimers.

One possible consequence of the alternative complex formation of MBW proteins is the temporal regulation of downstream genes. This scenario can be derived from the temporal-spatial expression patterns of *GL1*, *GL3*, and *TTG1* in leaves. In the trichome-patterning regions of young leaves, all three MBW genes are expressed ubiquitously in all cells (Larkin et al., 1993; Zhang et al., 2003; Bouyer et al., 2008; Zhao et al., 2008). Later, *GL1* and *GL3* expression increases in developing trichomes, whereas *TTG1* expression is more or less also ubiquitous during later stages (Larkin et al., 1993; Zhang et al., 2003; Bouyer et al., 2008; Zhao et al., 2008). Therefore, one would expect that the relative concentrations of *GL3*, *GL1* and *GL3* *TTG1* change during the patterning process such that, at later stages, *GL3* and *GL1* are more prominent in developing trichomes than *TTG1*. As a consequence, genes activated by *GL3* and *GL1* should be expressed successively more strongly than those regulated by *GL3* and *TTG1* during the course of trichome development.

## Perspectives

Our finding that the MBW proteins can also act as two alternative dimers sheds new light on the regulation schemes they are involved in and will require their experimental reassessment. For patterning processes, such a reevaluation will require a systematic analysis of the regulation scheme of all genes involved to understand the regulatory network. Modeling approaches may help to understand the possible relevance of differential regulation as sketched above for *CPC* and *TRY*. Finally, our results raise questions about the relevance of the alternative complex formation of MBW proteins and their R3MYB inhibitors during evolution.

## MATERIALS AND METHODS

### Plant Lines and Growth Conditions

*Arabidopsis* (*Arabidopsis thaliana*) plants were grown on soil at 24°C with 16 h of light per day. Plant transformations were performed by the floral dip method (Clough and Bent, 1998). In this study, we used either the wild-type Landsberg *erecta* or Columbia-0. Dark-grown cell suspension culture generated from roots of *Arabidopsis* Columbia-0 was established as described before (Gigolashvili et al., 2007). To determine anthocyanin production, plants were grown for 5 d on 1% (w/v) Murashige and Skoog medium at 22°C with 16 h of light per day ( $120 \pm 10 \mu\text{mol m}^{-2} \text{s}^{-1}$ ).

### Constructs

All CDS entry clones were generated by amplifying the CDSs from start to stop codon on *Arabidopsis* Landsberg *erecta* total complementary DNA synthesized from total vegetative green plant tissue and cloning in pENTR1A/pENTR4 or BP recombination in pDONR201. Mutated entry clones of *TRY*, *CPC*, and *GL1* were created by site-directed mutagenesis.

### Yeast Vectors

Fusions of the CDSs to the GAL4 binding domain of TTG1, TTG1Δ26 (last 26 amino acids are deleted to prevent interaction with GL3; Payne et al., 2000), GL1Δ27 (last 27 amino acids are deleted to prevent self-activation; Kirik et al., 2005), GL1Δ27-L86A, GL1Δ27-R97A, GL1Δ27-R97D, TRY, CPC, and TTG1 were produced in pAS-attR through LR reaction. As a negative control, the vector pAS-attR was recombined with pENTR1A-*w/o-ccdB*. The CDSs of GL3, TTG1, GL1, GL1Δ27, WER, TRY, and CPC were fused to the CDS for the GAL4 activation domain via LR in pC-ACT2-attR. As a negative control, the vector pC-ACT2-attR was recombined with pENTR1A-*w/o-ccdB*.

For the yeast three-hybrid analysis, we used pBRIDGE-attR. This was created by cloning the Gateway recombination cassette reading frame A into the blunted *NotI* *Bgl*III restriction sites of pBRIDGE (Clontech). This vector enables the expression of a third gene of interest (*GL1Δ27*, *GL1Δ27-R97D*, *TTG1*, or *TTG1Δ26*) under the control of the Met-repressible promoter pMet-25. As a control, the vector pBRIDGE-attR was recombined with pENTR1A-*w/o-ccdB*. A second protein (GL1Δ27, GL1Δ27-L86A, TTG1, or TTG1Δ26) was fused to the GAL4 binding domain under the control of the ubiquitous alcohol dehydrogenase promoter.

To test all MYB factors in the yeast three-hybrid system, we modified pYEA (Sandrock et al., 2001) by introducing the Gateway recombination cassette of pBluescript-GW-RekA. pYEA-attR was recombined with the respective entry clones for *GL1Δ27*, *WER*, *TRY*, *CPC*, and *GL1Δ27-R97D*. As a negative control, the vector pYEA-attR was recombined with pENTR1A-*w/o-ccdB*.

### Plant Vectors

N-terminal YFP and CFP fusions were created by recombination of the corresponding entry clones and pENTR1A-*w/o-ccdB* with pENS-G-YFP, pENS-G-CFP (Feys et al., 2005), and pAM-PAT-GWPro35S (GenBank accession no. AY436765), respectively.

### Effector and Reporter Constructs for Transient Cotransformation Experiments in Arabidopsis Cell Suspension Culture

To drive the expression of the *GUS* gene under the control of the *TRY* or *CPC* promoter, the binary plant transformation vector pGWB3i containing an intron within the *GUS* gene was used after recombination with the previously described promoter fragments (Gigolashvili et al., 2007; Pesch and Hülskamp, 2011). The effector constructs (35S:GL3, 35S:TTG1, 35S:TTG1Δ26, 35S:GL1, 35S:GL1-R97D, 35S:TRY, 35S:CPC, and 35S:WER) were also created by LR recombinations of the respective entry clones with pGWB2. For the empty control construct without CDS, pGWB2 was recombined with pENTR1A-*w/o-ccdB*.

### LUMIER Vectors

Three different destination vectors were used for subsequent LR reactions. pcDNA3-Rluc-GW and pTREXdest30 (Invitrogen) enable the N-terminal fusion of *Renilla reniformis* and *Staphylococcus aureus* proteins, respectively, and were described before (Pesch et al., 2013). pTREX-dest30re enables unfused protein expression.

GL1, WER, TRY, CPC, GL3, TTG1, and TTG1Δ26 were N terminally fused to the *S. aureus* ProtA sequence in pTREX-dest30-ntPrA by LR reaction. As a negative control, the vector pTREX-dest30-ntPrA was recombined with pENTR1A-*w/o-ccdB*.

*R. reniformis* Luciferase-GL3, Luciferase-TTG1, Luciferase-GL1, Luciferase-WER, Luciferase-TT2, Luciferase-CPC, Luciferase-GL1-R97D, and Luciferase-TRY were generated by LR reaction, fusing the full-length *R. reniformis* luciferase sequence N terminally to the CDSs in pcDNA3-Rluc-GW. Also, pENTR1A-*w/o-ccdB* was recombined to this vector as a negative control.

Untagged TTG1, TTG1Δ26, GL1, GL1-R97D, WER, TRY, CPC, and the control without any CDS were created by LR recombination of pTREX-dest30re with the respective entry clones.

## Molecular Biology Methods

### RNA Extraction and Real-Time PCR

Total RNA was extracted from *Arabidopsis* dark-grown cell suspension culture using the Qiagen RNasy Plant Mini Kit. After DNase treatment (Thermo Scientific), 1.5 μg of total RNA was used for reverse transcription (Thermo Scientific First Strand cDNA Synthesis Kit). Real-time PCR was performed using

the SYBR Green Real-Time PCR Master Mix (Applied Biosystems). Transcript levels of the analyzed genes were normalized to 18S ribosomal RNA (Zhang et al., 2012). Each experiment was averaged from three biological replicates, each represented by two technical replicates. Published and newly designed primers are listed in Supplemental Table S3 (Zhao et al., 2008; Zhang et al., 2012; Rishmawi et al., 2014).

### Cotransformation Assays in Arabidopsis Cell Suspension Culture and GUS Activity Assay

Dark-grown Arabidopsis cell suspension culture was transfected with different combinations of the effector constructs (35S promoter with the different CDSs in pGWB2) and the reporter construct *pTRY::GUS* or *pCPC::GUS* in pGWB3i. Each effector construct and the promoter *GUS* construct were separately transformed in the supervirulent *Agrobacterium tumefaciens* strain LBA4404.pBBR1MCS.virGN54D (kindly provided by J. Memelink, University of Leiden, through T. Gigolashvili) and together with *A. tumefaciens* strain RK19 containing the antisilencing 19 K protein (Voinnet et al., 1999) used for transformation. To ensure comparability in one set of experiments, the following measures were taken. All *A. tumefaciens* cultures were grown under exactly the same conditions. A combination of the different *A. tumefaciens* cultures for transformation was mixed in advance and then added to each of the three replicates of the cell culture samples. The same number of added *A. tumefaciens* cultures for transformation was always used in one set of experiments. This means that when unequal amounts of effectors were incurred by different approaches, the missing volumes were made up with an equivalent volume of *A. tumefaciens* resuspended culture containing the pGWB2-*ccdB-w/o* construct without any CDS.

Cell cultures were incubated on six-well plates at 22°C and 120 rpm in the dark for 5 d, pelleted, and frozen in liquid nitrogen. Protein crude extracts were prepared, and the protein concentrations were determined (BCA Protein Assay Kit; Pierce). GUS activity was determined by measuring the turnover of the 4-methylumbelliferyl  $\beta$ -D-glucuronide substrate for each sample using sample duplicates. 4-Methylumbelliferone production was determined fluorometrically (excitation, 365 nm; emission, 455 nm) every 15 min for 4 h using the Tecan Infinite 200 Titerplate reader and Tecan i-Control 1.4.5.0 software. 4-Methylumbelliferone production per min was correlated to the total protein amount, and mean values and SD of the three parallel samples were calculated.

### Yeast Two-Hybrid and Yeast Three-Hybrid Assays

The yeast two-hybrid assays were performed through cotransformation of the respective prey and bait vectors in the yeast (*Saccharomyces cerevisiae*) strain AH109 according to the previously described lithium acetate transformation method (Gietz et al., 1995).

The transformed yeast cells were selected by plating them onto synthetic dropout selection medium lacking Leu and Trp. Interactions were assayed on synthetic dropout interaction medium lacking Leu, Trp, and His (SD-LWH). The stringency of the interaction was tested by the addition of different concentrations of 3-aminotriazole. For all hybrid bait proteins, we excluded self-activation.

For the yeast three-hybrid assay, the prey vector pC-ACT2-GL3 was cotransformed with the different pBRIDGE bait vectors in the yeast strain AH109. Transformed cells were selected on synthetic dropout selection medium lacking Leu and Trp and interactions on SD-LWH. The effect of the third protein tested for its competition ability was compared by plating on SD-LWH plates also lacking Met (highest expression of the third protein) or on SD-LWH plates supplemented with different concentrations of Met. The specificity of the stringency of the assay was tested by adding 25 mM 3-aminotriazole.

For the  $\alpha$ -galactosidase assays, liquid precultures in SD-LWH were inoculated with five yeast colonies and incubated overnight. Triplicates of each approach were diluted and grown for 16 h. To determine the Met dependency, the precultures were diluted in SD-LWH medium supplemented with different concentrations of Met (0, 10, 25, 50, and 100  $\mu$ M). Afterward, the optical density at 600 nm was recorded. The calorimetric  $\alpha$ -galactosidase assay of the supernatant and the following activity calculation were done as described in the Clontech Yeast Protocols Handbook.

To test the different MYB factors in yeast three-hybrid assays, pC-ACT2-GL3 was cotransformed with pAS-TTG1 and the pYEA vector (*GL1 $\Delta$ 27*, *WER*, *TRY*, *CPC*, or *ccdB-w/o*) in the yeast strain Y190 and selected by plating onto synthetic dropout medium lacking Leu, Trp, and adenine.

### LUMIER

For LUMIER assays, each protein was transiently expressed in HEK293TN cells (BioCat/SBI; LV900A-1) as untagged proteins or as hybrid proteins either with *S. aureus* ProtA or *R. reniformis* Luciferase fused to their N termini.

Transfection and cell harvesting were done as described before (Pesch et al., 2013). After 48 h, the medium was removed; cells were washed three times with phosphate-buffered saline and collected in phosphate-buffered saline to a final volume of 1,000  $\mu$ L per well. *R. reniformis* Luciferase-GL3 (200  $\mu$ L)-expressing cells and 200  $\mu$ L of *S. aureus* ProtA-GL1-, ProtA-TTG1-, or ProtA-TTG1 $\Delta$ 26-expressing cells were mixed with 300  $\mu$ L of untagged protein-expressing cells according to Supplemental Table S4. Each combination was prepared in triplicate. Lysis of the combined cells with 50  $\mu$ L of lysis buffer, protein immunoprecipitation with sheep anti-rabbit IgG-coated magnetic beads in a magnetic holder, and luminescence measurement after pulldown in a microtiter plate reader were done as described previously (Pesch et al., 2013). The pulldown was also performed with untransfected cells or with cells solely expressing Luciferase-GL3 to exclude any nonspecific signal from the cell lysate or nonspecific binding of Luciferase-GL3 to the beads, respectively.

### FLIM-FRET Analysis

Tobacco (*Nicotiana tabacum*) leaves were transiently transformed by *A. tumefaciens* infiltration using the strain GV3101 pMP90RK coinfiltrated with the anti-silencing strain RK19 (Voinnet et al., 1999). The pENS-G-YFP, pENS-G-CFP, and pAM-PAT-Pro<sub>35S</sub> vectors containing the CDS of the respective genes were used. Two days after the transformation procedure, the samples were used for FLIM.

FLIM was performed on a confocal laser-scanning microscope (Zeiss LSM 780) additionally equipped with a single-photon-counting device with picosecond time resolution (PicoQuant Hydra Harp 400). CFP fluorescence was excited at 440 nm using a linearly polarized diode laser (LDH-D-C-440) operated at a repetition rate of 32 MHz. Excitation power was below 1  $\mu$ W at objective (40 $\times$  water immersion, numerical aperture 1.2; Zeiss C-PlanApo). The emitted light was collected in the same objective and separated into its perpendicular and parallel polarization (PBS 101; Thorlabs). Fluorescence was then detected by Tau-SPADs (PicoQuant) in a narrow range of the CFP emission spectrum (band-pass filter HC480/40 AHF). Images were taken with 12.6- $\mu$ s pixel time and a resolution of 96 nm per pixel (Zoom10; 256  $\times$  256). A series of 60 frames were merged into one image and analyzed further (Widengren et al., 2006).

The fluorescence lifetime of CFP was determined and analyzed pixel-wise in merged images to increase photon numbers for analysis using the software tools AnI-3SF and Margarita (Software Package for Multiparameter Fluorescence Spectroscopy, Full Correlation, and Multiparameter Fluorescence Imaging [http://www.mpc.hhu.de/software.html] for Multiparameter Fluorescence Image Spectroscopy; Kudryavtsev et al., 2007; Weidtkamp-Peters et al., 2009). In fluorescence lifetime microscopy with high spatial resolution and low excitation power to prevent photobleaching, the number of photons per pixel is exceptionally low, ranging from 100 to 2,000 photons per pixel. Therefore, a model to fit the data with a minimal number of parameters has to be applied in conjunction with a maximum likelihood estimator (Schaffer et al., 1999; Eggeling et al., 2001; Widengren et al., 2006; Weidtkamp-Peters et al., 2009; Sisamakakis et al., 2010). We are aware that CFP alone already has a multiexponential fluorescence decay (Villoing et al., 2008), which becomes even more complex in the presence of additional FRET species. This generally multiexponential decay is approximated in the subsequent fluorescence lifetime analysis by a fluorescence-weighted average lifetime,  $t$ . Therefore, we used a monoexponential model function with two variables (fluorescence lifetime  $t$  and scatter contribution  $g$ ), as described elsewhere (Stahl et al., 2013), fitted with a maximum likelihood estimator. The instrument response function was measured using the dye erythrosine, which exhibits a very short fluorescence lifetime, which is additionally quenched in an aqueous, saturated potassium iodide solution. This approach delivers the average fluorescence lifetime as a stable parameter even in critical surroundings with high background and low expression levels.

Accession numbers are as follows: *CPC* (AT2G46410), *EGL3* (AT1G63650), *GL1* (AT3G27920), *GL3* (AT5G41315), *TRY* (AT5G53200), and *TTG1* (AT5G24520).

### Supplemental Data

The following supplemental materials are available.

**Supplemental Figure S1.** Mean fluorescence lifetime of CFP-GL1 and CFP\* in combination with YFP.

**Supplemental Figure S2.** Relative mRNA expression levels of *ACTIN*, *GL1*, *WER*, *MYB23*, *GL3*, *EGL3*, and *TTG1* in Arabidopsis dark cell suspension culture.

**Supplemental Table S1.** Mutant versions of *GL1* and *TTG1*.

**Supplemental Table S2.** Pulldown of dimeric complexes with the LUMIER technology.

**Supplemental Table S3.** Primer sequences.

**Supplemental Table S4.** LUMIER assay combination scheme.

## ACKNOWLEDGMENTS

We thank B. Kernebeck and I. Klinkhammer for excellent technical assistance and S. Schellmann (all Botanical Institute, University of Cologne) for critically reading the article. The following vectors and primers were kindly provided as indicated: pAMPAT-GW by Bekir Ülker (MPIZ); pGWB2 and pGWB3 by Tsuyoshi Nakagawa (Shimane University); pGWB3i vector by Bettina Berger and Tamara Givolashvili (Botanical Institute of Cologne); pBluescript-GW-RekA by S. Biere (MPIZ); *TRY*, *CPC*, *GL3*, *TTG1*, and entry clones by Ulrich Herrmann (UiT, Norway); pENTR1A-w/o-ccdB by Arp Schnittger (Hamburg University); *GL1*, *MYB23*, *GL3*, *EGL3*, and *TTG1* primers for quantitative PCR by Alexandra Steffens (University of Cologne); and TTG1Δ26 entry clone by Rachappa Balkunde (Cold Spring Harbor Laboratory).

Received March 3, 2015; accepted April 26, 2015; published April 29, 2015.

## LITERATURE CITED

- Balkunde R, Bouyer D, Hülskamp M (2011) Nuclear trapping by GL3 controls intercellular transport and redistribution of TTG1 protein in Arabidopsis. *Development* **138**: 5039–5048
- Balkunde R, Pesch M, Hülskamp M (2010) Trichome patterning in Arabidopsis thaliana from genetic to molecular models. *Curr Top Dev Biol* **91**: 299–321
- Barrios-Rodiles M, Brown KR, Ozdamar B, Bose R, Liu Z, Donovan RS, Shinjo F, Liu Y, Dembowy J, Taylor IW, et al (2005) High-throughput mapping of a dynamic signaling network in mammalian cells. *Science* **307**: 1621–1625
- Baudry A, Heim MA, Dubreucq B, Caboche M, Weisshaar B, Lepiniec L (2004) TT2, TT8, and TTG1 synergistically specify the expression of BANYULS and proanthocyanidin biosynthesis in Arabidopsis thaliana. *Plant J* **39**: 366–380
- Berger F, Haseloff J, Schiefelbein J, Dolan L (1998) Positional information in root epidermis is defined during embryogenesis and acts in domains with strict boundaries. *Curr Biol* **8**: 421–430
- Bernhardt C, Lee MM, Gonzalez A, Zhang F, Lloyd A, Schiefelbein J (2003) The bHLH genes GLABRA3 (GL3) and ENHANCER OF GLABRA3 (EGL3) specify epidermal cell fate in the Arabidopsis root. *Development* **130**: 6431–6439
- Bernhardt C, Zhao M, Gonzalez A, Lloyd A, Schiefelbein J (2005) The bHLH genes GL3 and EGL3 participate in an intercellular regulatory circuit that controls cell patterning in the Arabidopsis root epidermis. *Development* **132**: 291–298
- Bouyer D, Geier F, Kragler F, Schnittger A, Pesch M, Wester K, Balkunde R, Timmer J, Fleck C, Hülskamp M (2008) Two-dimensional patterning by a trapping/depletion mechanism: the role of TTG1 and GL3 in Arabidopsis trichome formation. *PLoS Biol* **6**: e141
- Broun P (2005) Transcriptional control of flavonoid biosynthesis: a complex network of conserved regulators involved in multiple aspects of differentiation in Arabidopsis. *Curr Opin Plant Biol* **8**: 272–279
- Clough S, Bent A (1998) Floral dip: a simplified method for Agrobacterium-mediated transformation of Arabidopsis thaliana. *Plant J* **16**: 735–743
- Di Cristina M, Sessa G, Dolan L, Linstead P, Baima S, Ruberti I, Morelli G (1996) The Arabidopsis Athb-10 (GLABRA2) is an HD-Zip protein required for regulation of root hair development. *Plant J* **10**: 393–402
- Digiuni S, Schellmann S, Geier F, Greesse B, Pesch M, Wester K, Dartan B, Mach V, Srinivas BP, Timmer J, et al (2008) A competitive complex formation mechanism underlies trichome patterning on Arabidopsis leaves. *Mol Syst Biol* **4**: 217
- Eggeling C, Berger S, Brand L, Fries JR, Schaffer J, Volkmer A, Seidel CA (2001) Data registration and selective single-molecule analysis using multi-parameter fluorescence detection. *J Biotechnol* **86**: 163–180
- Esch JJ, Chen M, Sanders M, Hillestad M, Ndkium S, Idelkope B, Neizer J, Marks MD (2003) A contradictory GLABRA3 allele helps define gene interactions controlling trichome development in Arabidopsis. *Development* **130**: 5885–5894
- Feller A, Hernandez JM, Grotewold E (2006) An ACT-like domain participates in the dimerization of several plant basic-helix-loop-helix transcription factors. *J Biol Chem* **281**: 28964–28974
- Feller A, Machemer K, Braun EL, Grotewold E (2011) Evolutionary and comparative analysis of MYB and bHLH plant transcription factors. *Plant J* **66**: 94–116
- Feys BJ, Wiermer M, Bhat RA, Moisan LJ, Medina-Escobar N, Neu C, Cabral A, Parker JE (2005) Arabidopsis SENESCENCE-ASSOCIATED GENE101 stabilizes and signals within an ENHANCED DISEASE SUSCEPTIBILITY1 complex in plant innate immunity. *Plant Cell* **17**: 2601–2613
- Gan L, Xia K, Chen JG, Wang S (2011) Functional characterization of TRICHOMELESS2, a new single-repeat R3 MYB transcription factor in the regulation of trichome patterning in Arabidopsis. *BMC Plant Biol* **11**: 176
- Gietz RD, Schiestl RH, Willems AR, Woods RA (1995) Studies on the transformation of intact yeast cells by the LiAc/SS-DNA/PEG procedure. *Yeast* **11**: 355–360
- Gigolashvili T, Berger B, Mock HP, Müller C, Weisshaar B, Flügge UI (2007) The transcription factor HIG1/MYB51 regulates indolic glucosinolate biosynthesis in Arabidopsis thaliana. *Plant J* **50**: 886–901
- Hülskamp M, Misra S, Jürgens G (1994) Genetic dissection of trichome cell development in Arabidopsis. *Cell* **76**: 555–566
- Hung CY, Lin Y, Zhang M, Pollock S, Marks MD, Schiefelbein J (1998) A common position-dependent mechanism controls cell-type patterning and GLABRA2 regulation in the root and hypocotyl epidermis of Arabidopsis. *Plant Physiol* **117**: 73–84
- Kirik V, Lee MM, Wester K, Herrmann U, Zheng Z, Oppenheimer D, Schiefelbein J, Hülskamp M (2005) Functional diversification of MYB23 and GL1 genes in trichome morphogenesis and initiation. *Development* **132**: 1477–1485
- Kirik V, Schnittger A, Radchuk V, Adler K, Hülskamp M, Bäumlein H (2001) Ectopic expression of the Arabidopsis AtMYB23 gene induces differentiation of trichome cells. *Dev Biol* **235**: 366–377
- Kirik V, Simon M, Huelskamp M, Schiefelbein J (2004a) The ENHANCER OF TRY AND CPC1 gene acts redundantly with TRIPTYCHON and CAPRICE in trichome and root hair cell patterning in Arabidopsis. *Dev Biol* **268**: 506–513
- Kirik V, Simon M, Wester K, Schiefelbein J, Hülskamp M (2004b) ENHANCER OF TRY AND CPC 2 (ETC2) reveals redundancy in the region-specific control of trichome development of Arabidopsis. *Plant Mol Biol* **55**: 389–398
- Koes R, Verweij W, Quattrocchio F (2005) Flavonoids: a colorful model for the regulation and evolution of biochemical pathways. *Trends Plant Sci* **10**: 236–242
- Koornneef M (1981) The complex syndrome of *ttg* mutants. *Arabidopsis Inf Serv* **18**: 45–51
- Kudryavtsev V, Felekyan S, Woźniak AK, König M, Sandhagen C, Kühnemuth R, Seidel CA, Oesterhelth F (2007) Monitoring dynamic systems with multiparameter fluorescence imaging. *Anal Bioanal Chem* **387**: 71–82
- Larkin JC, Oppenheimer DG, Pollock S, Marks MD (1993) Arabidopsis GLABROUS1 gene requires downstream sequences for function. *Plant Cell* **5**: 1739–1748
- Lee MM, Schiefelbein J (1999) WEREWOLF, a MYB-related protein in Arabidopsis, is a position-dependent regulator of epidermal cell patterning. *Cell* **99**: 473–483
- Lepiniec L, Debeaujon I, Routaboul JM, Baudry A, Pourcel L, Nesi N, Caboche M (2006) Genetics and biochemistry of seed flavonoids. *Annu Rev Plant Biol* **57**: 405–430
- Masucci JD, Rerie WG, Foreman DR, Zhang M, Galway ME, Marks MD, Schiefelbein JW (1996) The homeobox gene GLABRA2 is required for position-dependent cell differentiation in the root epidermis of Arabidopsis thaliana. *Development* **122**: 1253–1260
- Morohashi K, Grotewold E (2009) A systems approach reveals regulatory circuitry for Arabidopsis trichome initiation by the GL3 and GL1 selectors. *PLoS Genet* **5**: e1000396
- Morohashi K, Zhao M, Yang M, Read B, Lloyd A, Lamb R, Grotewold E (2007) Participation of the Arabidopsis bHLH factor GL3 in trichome initiation regulatory events. *Plant Physiol* **145**: 736–746
- Oppenheimer DG, Herman PL, Sivakumaran S, Esch J, Marks MD (1991) A *myb* gene required for leaf trichome differentiation in Arabidopsis is expressed in stipules. *Cell* **67**: 483–493



- Payne CT, Zhang F, Lloyd AM (2000) GL3 encodes a bHLH protein that regulates trichome development in Arabidopsis through interaction with GL1 and TTG1. *Genetics* **156**: 1349–1362
- Pesch M, Dartan B, Birkenbihl R, Somssich IE, Hülskamp M (2014) Arabidopsis TTG2 regulates TRY expression through enhancement of activator complex-triggered activation. *Plant Cell* **26**: 4067–4083
- Pesch M, Hülskamp M (2011) Role of TRIPTYCHON in trichome patterning in Arabidopsis. *BMC Plant Biol* **11**: 130
- Pesch M, Schultheiß I, Digiuni S, Uhrig JF, Hülskamp M (2013) Mutual control of intracellular localisation of the patterning proteins ATMYC1, GL1 and TRY/CPC in Arabidopsis. *Development* **140**: 3456–3467
- Ramsay NA, Glover BJ (2005) MYB-bHLH-WD40 protein complex and the evolution of cellular diversity. *Trends Plant Sci* **10**: 63–70
- Rerie WG, Feldmann KA, Marks MD (1994) The GLABRA2 gene encodes a homeo domain protein required for normal trichome development in Arabidopsis. *Genes Dev* **8**: 1388–1399
- Rishmawi L, Sun H, Schneeberger K, Hülskamp M, Schrader A (2014) Rapid identification of a natural knockout allele of *ARMADILLO REPEAT-CONTAINING KINESIN1* that causes root hair branching by mapping-by-sequencing. *Plant Physiol* **166**: 1280–1287
- Sandrock B, Tirode F, Egly JM (2001) Three-hybrid screens: inducible third-party systems. *Methods Mol Biol* **177**: 271–289
- Schaffer J, Volkmer A, Eggeling C, Subramaniam V, Striker G, Seidel C (1999) Identification of single molecules in aqueous solution by time-resolved fluorescence anisotropy. *J Phys Chem A* **103**: 331–336
- Schellmann S, Schnittger A, Kirik V, Wada T, Okada K, Beermann A, Thumfahrt J, Jürgens G, Hülskamp M (2002) TRIPTYCHON and CAPRICE mediate lateral inhibition during trichome and root hair patterning in Arabidopsis. *EMBO J* **21**: 5036–5046
- Serna L, Martin C (2006) Trichomes: different regulatory networks lead to convergent structures. *Trends Plant Sci* **11**: 274–280
- Simon M, Lee MM, Lin Y, Gish L, Schiefelbein J (2007) Distinct and overlapping roles of single-repeat MYB genes in root epidermal patterning. *Dev Biol* **311**: 566–578
- Sisamakris E, Valeri A, Kalinin S, Rothwell PJ, Seidel CA (2010) Accurate single-molecule FRET studies using multiparameter fluorescence detection. *Methods Enzymol* **475**: 455–514
- Stahl Y, Grabowski S, Bleckmann A, Kuhnemuth R, Weidtkamp-Peters S, Pinto KG, Kirschner GK, Schmid JB, Wink RH, Hulsewede A, et al (2013) Moderation of Arabidopsis root stemness by CLAVATA1 and ARABIDOPSIS CRINKLY4 receptor kinase complexes. *Curr Biol* **23**: 362–371
- Tominaga R, Iwata M, Okada K, Wada T (2007) Functional analysis of the epidermal-specific MYB genes CAPRICE and WEREWOLF in Arabidopsis. *Plant Cell* **19**: 2264–2277
- Tominaga R, Iwata M, Sano R, Inoue K, Okada K, Wada T (2008) Arabidopsis CAPRICE-LIKE MYB 3 (CPL3) controls endoreduplication and flowering development in addition to trichome and root hair formation. *Development* **135**: 1335–1345
- Tominaga-Wada R, Ishida T, Wada T (2011) New insights into the mechanism of development of Arabidopsis root hairs and trichomes. *Int Rev Cell Mol Biol* **286**: 67–106
- Villoing A, Ridhoir M, Cinquin B, Erard M, Alvarez L, Vallverdu G, Pernot P, Grailhe R, Mérola F, Pasquier H (2008) Complex fluorescence of the cyan fluorescent protein: comparisons with the H148D variant and consequences for quantitative cell imaging. *Biochemistry* **47**: 12483–12492
- Voinnet O, Pinto YM, Baulcombe DC (1999) Suppression of gene silencing: a general strategy used by diverse DNA and RNA viruses of plants. *Proc Natl Acad Sci USA* **96**: 14147–14152
- Wada T, Kurata T, Tominaga R, Koshino-Kimura Y, Tachibana T, Goto K, Marks MD, Shimura Y, Okada K (2002) Role of a positive regulator of root hair development, CAPRICE, in Arabidopsis root epidermal cell differentiation. *Development* **129**: 5409–5419
- Wada T, Tachibana T, Shimura Y, Okada K (1997) Epidermal cell differentiation in Arabidopsis determined by a Myb homolog, CPC. *Science* **277**: 1113–1116
- Walker AR, Davison PA, Bolognesi-Winfield AC, James CM, Srinivasan N, Blundell TL, Esch JJ, Marks MD, Gray JC (1999) The *TRANSPARENT TESTA GLABRA1* locus, which regulates trichome differentiation and anthocyanin biosynthesis in Arabidopsis, encodes a WD40 repeat protein. *Plant Cell* **11**: 1337–1350
- Wang S, Hubbard L, Chang Y, Guo J, Schiefelbein J, Chen JG (2008) Comprehensive analysis of single-repeat R3 MYB proteins in epidermal cell patterning and their transcriptional regulation in Arabidopsis. *BMC Plant Biol* **8**: 81
- Wang S, Kwak SH, Zeng Q, Ellis BE, Chen XY, Schiefelbein J, Chen JG (2007) TRICHOMELESS1 regulates trichome patterning by suppressing GLABRA1 in Arabidopsis. *Development* **134**: 3873–3882
- Weidtkamp-Peters S, Felekyan S, Bleckmann A, Simon R, Becker W, Kuhnemuth R, Seidel CA (2009) Multiparameter fluorescence image spectroscopy to study molecular interactions. *Photochem Photobiol Sci* **8**: 470–480
- Wester K, Digiuni S, Geier F, Timmer J, Fleck C, Hülskamp M (2009) Functional diversity of R3 single-repeat genes in trichome development. *Development* **136**: 1487–1496
- Widengren J, Kudryavtsev V, Antonik M, Berger S, Gerken M, Seidel CA (2006) Single-molecule detection and identification of multiple species by multiparameter fluorescence detection. *Anal Chem* **78**: 2039–2050
- Zhang F, Gonzalez A, Zhao M, Payne CT, Lloyd A (2003) A network of redundant bHLH proteins functions in all TTG1-dependent pathways of Arabidopsis. *Development* **130**: 4859–4869
- Zhang H, Deng X, Miki D, Cutler S, La H, Hou YJ, Oh J, Zhu JK (2012) Sulfamethazine suppresses epigenetic silencing in Arabidopsis by impairing folate synthesis. *Plant Cell* **24**: 1230–1241
- Zhao M, Morohashi K, Hatlestad G, Grotewold E, Lloyd A (2008) The TTG1-bHLH-MYB complex controls trichome cell fate and patterning through direct targeting of regulatory loci. *Development* **135**: 1991–1999
- Zimmermann IM, Heim MA, Weisshaar B, Uhrig JF (2004) Comprehensive identification of Arabidopsis thaliana MYB transcription factors interacting with R/B-like BHLH proteins. *Plant J* **40**: 22–34